


Article

Structure-Preserving Numerical Methods for Fractional Nonlinear Schrödinger Equations with Wave Operators

Mengnan Zhang , Xinyu Zhou and Cuicui Liao *

College of Science, Jiangnan University, Wuxi 214122, China; 6231204018@stu.jiangnan.edu.cn (M.Z.); 6241204023@stu.jiangnan.edu.cn (X.Z.)

* Correspondence: cliao@jiangnan.edu.cn

Abstract

This main focus of this work is the fractional-order nonlinear Schrödinger equation with wave operators. First, a conservative difference scheme is constructed. Then, the discrete energy and mass conservation formulas are derived and maintained by the difference scheme constructed in this paper. Through rigorous theoretical analysis, it is proved that the constructed difference scheme is unconditionally stable and has second-order precision in both space and time. Due to the completely implicit property of the differential scheme proposed, a linearized iterative algorithm is proposed to implement the conservative differential scheme. Numerical experiments including one example with the fractional boundary conditions were studied. The results effectively demonstrate the long-term numerical behaviors of the fractional nonlinear Schrödinger equations with wave operators.

Keywords: fractional Schrödinger equation; energy-conserving methods; conservation laws; wave operators; convergence; stability

MSC: 35Q55; 65M06; 65M12



Received: 9 September 2025
Revised: 22 September 2025
Accepted: 29 September 2025
Published: 5 October 2025

Citation: Zhang, M.; Zhou, X.; Liao, C. Structure-Preserving Numerical Methods for Fractional Nonlinear Schrödinger Equations with Wave Operators. *Mathematics* **2025**, *13*, 3187. <https://doi.org/10.3390/math13193187>

Copyright: © 2025 by the authors. Licensee MDPI, Basel, Switzerland. This article is an open access article distributed under the terms and conditions of the Creative Commons Attribution (CC BY) license (<https://creativecommons.org/licenses/by/4.0/>).

1. Introduction

The Schrödinger equation, as the core equation of quantum mechanics, describes the spatial distribution and temporal evolution of the wave function of microscopic particles. However, particle dynamics in fractal media, anomalous diffusion, or long-range interaction systems are difficult to accurately classify with classical models [1]. In recent years, the wave-type fractional Schrödinger equation (WFSE) with wave operators has been proposed. The WFSE combines the non-locality of fractional derivatives with the second-order temporal characteristics of wave operators, providing a more universal mathematical framework for wave propagation in complex quantum systems and non-local media [2,3]. It has been applied in many scientific fields, such as modeling soliton transmission in optical fiber communication [4,5] and ultra-cold atomic gases and superfluids in non-local quantum systems [6–8]. More specifically, the wave-type fractional Schrödinger equation has been utilized to describe the non-Markovian dynamics of open quantum systems with memory effects [9,10], the propagation of laser beams in nonlinear fractional media with long-range interactions, and the study of wave scattering in fractal porous materials where the fractional order α is linked to the fractal dimension of the material [11,12].

In this paper, we discuss the nonlinear fractional Schrödinger equation with wave operators as follows [13]:

$$\psi_{tt}(x, t) + (-\Delta)^{\alpha/2} \psi(x, t) + i\gamma \psi_t(x, t) + \beta |\psi(x, t)|^2 \psi(x, t) = 0, \quad a < x < b, 0 < t < T, \quad (1)$$

with the initial condition:

$$\psi(x, 0) = \psi_0(x), \quad \psi_t(x, 0) = \psi_1(x), \quad (2)$$

and the Dirichlet boundary condition:

$$\psi(a, t) = \psi(b, t) = 0, \quad 0 \leq t \leq T, \quad (3)$$

where $i = \sqrt{-1}$, $p \in \mathbb{Z}^+$, $1 < \alpha \leq 2$, α are positive real constants; the parameter β is a real constant; $\psi(x, t)$ is a complex-valued wave function with periodic boundary conditions; and $\psi_0(x)$, $\psi_1(x)$ are given smooth initial value functions.

The spatial fractional Laplace operator [14] is used to characterize the non-local motion of particles in fractal media, simulating the anomalous diffusion and long-range correlation effects of particles in disordered media such as optical lattices [15]. It has multiple equivalent definitions in \mathbb{R} , such as Riesz, spectral, and directional definitions. However, when these definitions are limited to bounded regions, the relevant boundary conditions can lead to different operator forms [16,17]. The Ritz fractional derivatives are studied in this paper and are defined as

$$(-\Delta)^{\frac{\alpha}{2}} \psi(x) = \frac{1}{2 \cos \frac{\alpha\pi}{2}} \left[{}_{-\infty}D_x^{\alpha} \psi(x, t) + {}_xD_{+\infty}^{\alpha} \psi(x, t) \right], \quad (4)$$

where ${}_{-\infty}D_x^{\alpha} \psi(x, t)$, ${}_xD_{+\infty}^{\alpha} \psi(x, t)$ represent the left- and right-side Riemann–Liouville fractional derivatives:

$${}_{-\infty}D_x^{\alpha} \psi(x, t) = \begin{cases} \frac{1}{\Gamma(2-\alpha)} \frac{d^2}{dx^2} \int_a^x (x-s)^{1-\alpha} \psi(s, t) ds, & 1 < \alpha < 2, \\ \frac{d^2}{dx^2} \psi(x, t), & \alpha = 2, \end{cases}$$

$${}_xD_{+\infty}^{\alpha} \psi(x, t) = \begin{cases} \frac{1}{\Gamma(2-\alpha)} \frac{d^2}{dx^2} \int_x^b (s-x)^{1-\alpha} \psi(s, t) ds, & 1 < \alpha < 2, \\ \frac{d^2}{dx^2} \psi(x, t), & \alpha = 2, \end{cases}$$

$\Gamma(\cdot)$ is gamma function. The Riesz fractional derivative can also be defined as [14]:

$$-(-\Delta)^{\frac{\alpha}{2}} \psi(x, t) = -\mathcal{F}^{-1}(|\xi|^{\alpha} \hat{\psi}(\xi, t)),$$

where \mathcal{F} is the Fourier transform.

The classical nonlinear partial differential equations have some physical quantities naturally derived from the physical environment, such as symplectic and multi-symplectic conservation laws and energy and mass conservation laws. Bao [18] deduced that a system (1) with periodic boundary conditions has the following conservation laws of mass and energy:

$$M(t) = M(0), \quad E(t) = E(0), \quad (5)$$

where

$$M(t) := \gamma \|\psi(x, t)\|_{L^2}^2 + 2 \operatorname{Im}(\psi_t(x, t), \psi(x, t)),$$

$$E(t) := \|\psi_t(x, t)\|_{L^2}^2 + \|(-\Delta)^{\alpha/4} \psi(x, t)\|_{L^2}^2 + \frac{\beta}{2} \|\psi(x, t)\|_{L^4}^4, \quad (6)$$

and

$$\|\psi_t(x, t)\|_{L^2}^2 = \int_{\Omega} |\psi_t(x, t)|^2 dx, \quad \|\psi(x, t)\|_{L^p}^p = \int_{\Omega} |\psi(x, t)|^p dx. \quad (7)$$

Structure-preserving methods are crucial for the long-term simulation of the fractional nonlinear Schrödinger equation with wave operators for two primary reasons. First, the conservation laws of mass and energy are fundamental physical properties inherent to the closed system described by Equations (1)–(3). A numerical scheme that preserves these discrete analogues ensures that the numerical solution respects the underlying physics, preventing unphysical numerical dissipation or blow-up that can occur with non-conservative schemes [9,10]. Second, from a numerical analysis perspective, these conservation laws provide a powerful tool for proving the unconditional stability of the scheme, as demonstrated in Theorem 4. This is especially important for the nonlinear and non-local problems studied here, where conventional stability analysis can be exceedingly difficult. The ability to perform accurate and stable long-term simulations is paramount for studying the evolutionary behavior of wave functions in quantum systems, making structure-preserving methods the preferred choice for this class of problems [18,19].

Stable dynamics ensure that the system does not spontaneously generate or annihilate energy during the evolution process [20] and can maintain the stability of the physical state. Therefore, the conservation law and unconditional stability of equations have become hot topics in recent years. In the past few years, scholars have studied various conservative and precise numerical methods, such as the Galerkin finite element method [21,22], spectrum method [23–25], collocation methods [26], and finite difference method [19,27–29]. In Reference [21], a conservative difference scheme is constructed for the nonlinear fractional order Schrödinger equation in space based on discretization using the Galerkin finite element method in space and the Crank–Nicolson method in time. In Reference [22], Li et al. studied a series of Galerkin finite element methods and discussed the conservation and convergence of discrete systems. Wang and Huang [19] constructed a conservative linearized difference scheme and an energy conserving Crank–Nicolson difference scheme for the nonlinear Riesz fractional order Schrödinger equation and analyzed the convergence of the l^∞ -norm. Wang [28] used the compact difference method and extrapolation method to provide two high-order conservative difference schemes for fractional order derivatives and proved second-order accuracy convergence in both time and space.

This paper is structured as follows: In Section 2, various symbolic and discrete schemes for fractional derivatives are introduced. Section 3 presents a conservative difference scheme along with an iterative linearization algorithm. In Section 4, a detailed analysis of energy and mass conservation in discrete cases is conducted. Section 5 discusses the convergence and stability of the difference scheme. Numerical experiments are presented in Section 6. Finally, conclusions are drawn in Section 7.

2. Notations

We segment the region $[a, b] \times [0, T]$ with time step $\tau := \frac{T}{N}$ and space step $h := \frac{b-a}{M}$. The grid node is recorded as $\psi(x_j, t_n)$, where $x_j = j\Delta x$, $j = 0, 1, \dots, M$, and $t_n = n\Delta t$, $n = 0, 1, \dots, N$. Here, M, N is a positive integer. Let $\psi_j^n = \psi(x_j, t_n)$, $\psi_j^{*n} \approx \psi(x_j, t_n)$.

$$\Omega_h = \{x_j | 0 \leq j \leq M\}, \quad \Omega_\tau = \{t_n | 0 \leq n \leq N\}.$$

Given a grid function $w = \{w_j^n | (x_j, t_n) \in \Omega_h \times \Omega_\tau\}$, the finite difference operators can be defined:

$$\begin{aligned} \hat{w}_j^n &= \frac{w_j^{n+1} + w_j^{n-1}}{2}, & \delta_t w_j^n &= \frac{w_j^{n+1} - w_j^n}{\tau}, \\ \delta_t w_j^n &= \frac{w_j^{n+1} - w_j^{n-1}}{2\tau}, & \delta_t^2 w_j^n &= \frac{w_j^{n+1} - 2w_j^n + w_j^{n-1}}{\tau^2}. \end{aligned}$$

Let $\mathcal{V}_h = \{w \mid w = (w_1, \dots, w_{M-1})\}$ be the space of grid functions; for any grid function $u, v \in \mathcal{V}_h$, we define discrete inner product, L^2 -norm, and L^p -norm as

$$\begin{aligned}\langle u, v \rangle &= h \sum_{j=1}^{J-1} u_j \bar{v}_j, & \|u\|^2 &= \langle u, u \rangle, \\ \|u\|_h^p &= h \sum_{j=1}^{J-1} |u_j|^p, 1 \leq p < +\infty, & \|u\|_h^\infty &= \sup_{0 < j < J-1} |u_j|.\end{aligned}$$

This paper employs the fractional central difference discretization method for Riesz fractional derivatives. For $1 < \alpha < 2$, we define

$$-(-\Delta)^{\frac{\alpha}{2}} \psi_j^n = -\frac{1}{h^\alpha} \sum_{l=-M+j}^j g_l^{(\alpha)} \psi_{j-l}^n + O(h^2) = -\frac{1}{h^\alpha} \sum_{l=1}^{M-1} g_{j-l}^{(\alpha)} \psi_l^n + O(h^2), \quad (8)$$

where the coefficients $g_k^{(\gamma)} = \frac{(-1)^k \Gamma(\gamma+1)}{\Gamma(\frac{\gamma}{2}-k+1) \Gamma(\frac{\gamma}{2}+k+1)}$. For convenience, we introduce the following discrete operator:

$$\Delta_h^\alpha \psi_j^n = \frac{1}{h^\alpha} \sum_{k=1}^{M-1} g_{j-k}^{(\gamma)} \psi_k^n, \quad 1 \leq j \leq M-1. \quad (9)$$

Lemma 1. The coefficients $g_k^{(\alpha)}$ have the following properties (see [30]):

$$\begin{aligned}g_0^{(\gamma)} &\geq 0, \\ g_{-k}^{(\gamma)} &= g_k^{(\gamma)} \leq 0 \text{ for all } |k| \geq 1.\end{aligned} \quad (10)$$

Let

$$\Delta_h^\alpha \psi_j^{*n} = h^{-\alpha} \sum_{l=1}^{M-1} g_{j-l}^{(\alpha)} \psi_l^{*n}, \quad 1 \leq j \leq M-1.$$

where ψ_j^{*n} denotes the numerical approximation to ψ_j^n .

3. Conservative Difference Schemes

As stated in Lemma 1, the fractional central difference effectively preserves the symmetry properties of Riesz fractional derivatives, serving as a fundamental element in subsequent analysis. We define

$$\Delta_h^\alpha \psi(x_j, t_n) = (-\Delta)^{\frac{\alpha}{2}} \psi_j^n = -\frac{\partial^\alpha}{\partial |x|^\alpha} \psi(x, t) + O(h^2). \quad (11)$$

Let $\psi, \psi^* \in \mathcal{V}_h$ be the exact solution and numerical approximation, respectively. Considering the Schrödinger Equation (1) and using the Crank–Nicolson method in time and the fractional centered difference scheme (8) in space, we derive the conservative difference scheme for the Schrödinger equation, which is

$$\begin{aligned}\delta_t^2 \psi_j^{*n} + \Delta_h^\alpha \hat{\psi}_j^{*n} + i\gamma \delta_t \psi_j^{*n} + \frac{\beta}{2} (|\psi_j^{*(n-1)}|^2 + |\psi_j^{*(n+1)}|^2) \hat{\psi}_j^{*n} &= 0, 1 \leq j \leq M-1, 0 \leq n \leq N-1, \\ \psi_j^{*0} &= \psi_0(x_j), \quad \psi_t(x_j, 0) = \psi_1(x_j), \quad 0 \leq j \leq M, \\ \psi_0^{*n} &= \psi_M^{*n} = 0, \quad 0 \leq n \leq N.\end{aligned} \quad (12)$$

The above Equation (12) is divided into the following two cases:

(1) If $n = 0$,

$$(2 + \tau^2 \Delta_h^\alpha) \psi_j^{*1} = 2\psi_j^{*0} + (2\tau + \tau^3 \Delta_h^\alpha - i\gamma\tau^2) \psi_1(x_j) - \frac{\beta\tau^2}{2} (|\psi_j^{*1} - 2\tau\psi_1(x_j)|^2 + |\psi_j^{*1}|) (\psi_j^{*1} - \tau\psi_1(x_j)), \quad (13)$$

(2) If $n \geq 1$,

$$(1 + \frac{\tau^2}{2} \Delta_h^\alpha + \frac{i\alpha\tau}{2}) \psi_j^{*(n+1)} = 2\psi_j^{*n} + (-1 - \frac{\tau^2}{2} \Delta_h^\alpha + \frac{i\alpha\tau}{2}) \psi_j^{*(n-1)} - \frac{\beta\tau^2}{4} (|\psi_j^{*(n-1)}|^2 + |\psi_j^{*(n+1)}|^2) (\psi_j^{*(n+1)} + \psi_j^{*(n-1)}). \quad (14)$$

Given the characteristics of this numerical format in (13) and (14), MATLAB software (R2024a 9.8) is used in programming to obtain the values of each time layer through an iterative method; then, the following iterative algorithm is defined:

(1) If $n = 0$,

$$(2 + \tau^2 \Delta_h^\alpha) \psi_j^{*1(s+1)} = 2\psi_j^{*0} + (2\tau + \tau^3 \Delta_h^\alpha - i\gamma\tau^2) \psi_1(x_j) - \frac{\beta\tau^2}{2} (|\psi_j^{*1(s)} - 2\tau\psi_1(x_j)|^2 + |\psi_j^{*1(s)}|) (\psi_j^{*1(s)} - \tau\psi_1(x_j)), \quad (15)$$

(2) If $n \geq 1$,

$$(1 + \frac{\tau^2}{2} \Delta_h^\alpha + \frac{i\alpha\tau}{2}) \psi_j^{*(n+1)} = 2\psi_j^{*n} + (-1 - \frac{\tau^2}{2} \Delta_h^\alpha + \frac{i\alpha\tau}{2}) \psi_j^{*(n-1)} - \frac{\beta\tau^2}{4} (|\psi_j^{*(n-1)}|^2 + |\psi_j^{*(n+1)}|^2) (\psi_j^{*(n+1)} + \psi_j^{*(n-1)}). \quad (16)$$

where $1 \leq j \leq M-1$, $0 \leq n \leq N-1$, $s = 0, 1, 2, \dots$, and the initial iterations are given by

$$\psi_j^{*(n+1)(0)} = \begin{cases} \psi_j^{*n}, & n = 0, \\ 2\psi_j^{*n} - \psi_j^{*(n-1)}, & n \geq 1. \end{cases} \quad (17)$$

When $\|\psi_j^{*(n+1)(s+1)} - \psi_j^{*n}\|$ converges, the $\psi_j^{*(n+1)} = \psi_j^{*(n+1)(s+1)}$.

The computational cost per time step is dominated by solving the linear system with the dense Toeplitz matrix T_n . While a naive dense solver would incur a cost of $\mathcal{O}(M^3)$, the Toeplitz structure can be exploited using iterative solvers (e.g., Conjugate Gradient) coupled with Fast Fourier Transform for matrix–vector products, reducing the cost to $\mathcal{O}(M \log M)$ per iteration. The number of iterations in the linear solver and the outer fixed-point iteration (15) and (16) depends on the prescribed tolerance but is typically observed to be small and independent of the grid size in our numerical experiments.

4. Mass and Energy Conservation

The nonlinear fractional Schrödinger equation with wave operators (1)–(3) satisfies the conservation of energy and mass in the continuous sense. In this section, we will demonstrate that the difference scheme (12) preserves the conservation of energy and mass in the discrete setting.

Let the matrix T_n be

$$T_n = \begin{pmatrix} g_0^{(\gamma)} & g_{-1}^{(\gamma)} & \cdots & g_{-M+2}^{(\gamma)} \\ g_1^{(\gamma)} & g_0^{(\gamma)} & \cdots & g_{-M+3}^{(\gamma)} \\ \vdots & \vdots & \ddots & \vdots \\ g_{M-2}^{(\gamma)} & g_{M-3}^{(\gamma)} & \cdots & g_0^{(\gamma)} \end{pmatrix}. \quad (18)$$

It follows from $g_k^{(\gamma)} = g_{-k}^{(\gamma)}$ and Lemma 1 that the matrix T_n is a symmetric Toeplitz matrix. It is the discrete analogue of the fractional Laplacian operator $(-\Delta)^{\alpha/2}$ in the fractional central difference scheme. Its structure is central to proving the conservation properties and stability of our numerical method.

Denote $\lambda = [\lambda_1, \lambda_2, \dots, \lambda_{M-1}]$, where λ_i is the eigenvalue of matrix T_n .

Lemma 2. For any grid function $\psi^{*n}, \phi^{*n} \in \mathcal{V}_h$, there exists a linear operator Λ^α , such that (see [31]):

$$((-\Delta)^{\alpha/2} \psi^{*n}, \phi^{*n}) = (\Lambda^\alpha \psi^{*n}, \Lambda^\alpha \phi^{*n}). \quad (19)$$

Proof. There is a real orthogonal matrix P and a real diagonal matrix $A = \text{diag}(\lambda)$, such that

$$T_n = PAP^T = (PA^{\frac{1}{2}}P^T)^T(PA^{\frac{1}{2}}P^T) = Q^TQ,$$

where $A^{\frac{1}{2}} = \text{diag}(\lambda^{\frac{1}{2}})$, $Q = PA^{\frac{1}{2}}P^T$.

$$\begin{aligned} ((-\Delta)^{\alpha/2} \psi^{*n}, \phi^{*n}) &= (h^{-\alpha} T_n \psi^{*n}, \phi^{*n}) = (h^{-\alpha} Q^T Q \psi^{*n}, \phi^{*n}) \\ &= (h^{-\frac{\alpha}{2}} Q \psi^{*n}, h^{-\frac{\alpha}{2}} Q \phi^{*n}) = (\Lambda^\alpha \psi^{*n}, \Lambda^\alpha \phi^{*n}). \end{aligned}$$

where $\Lambda^\alpha \psi^{*n} = h^{-\frac{\alpha}{2}} Q \psi^{*n}$.

Thus, the proof is complete. \square

Lemma 3. For any grid function $\psi^{*n} \in \mathcal{V}_h$, we have

$$\begin{aligned} \text{Re}(\Delta_h^\alpha \hat{\psi}^{*n}, \delta_t \psi^{*n}) &= \frac{1}{4\tau} (\|\Lambda^\alpha \psi^{*(n+1)}\|^2 - \|\Lambda^\alpha \psi^{*(n-1)}\|^2), \\ \text{Re}(\delta_t^2 \psi^{*n}, \delta_t \psi^{*n}) &= \frac{1}{2\tau} (\|\delta_t \psi^{*n}\|^2 - \|\delta_t \psi^{*(n-1)}\|^2), \\ \text{Re}(\hat{\psi}^{*n}, \delta_t \psi^{*n}) &= \frac{1}{4\tau} (\|\psi^{*(n+1)}\|^2 - \|\psi^{*(n-1)}\|^2), \\ \text{Im}(\delta_t^2 \psi^{*n}, \hat{\psi}^{*n}) &= \frac{1}{\tau} (\text{Im}(\delta_t \psi^{*n}, \psi^{*n}) - \text{Im}(\delta_t \psi^{*(n-1)}, \psi^{*(n-1)})). \end{aligned} \quad (20)$$

Proof. This identity is proven by leveraging the self-adjointness and positive-definiteness of the discrete fractional operator established through Lemma 2. We substitute the definitions of the averaging and difference operators to express the inner product, which then simplifies to a difference of norms.

$$\begin{aligned} \text{Re}(\Delta_h^\alpha \hat{\psi}^{*n}, \delta_t \psi^{*n}) &= \text{Re}(\Lambda^\alpha \hat{\psi}^{*n}, \Lambda^\alpha \delta_t \psi^{*n}) \\ &= \frac{1}{4\tau} (\Lambda^\alpha (\psi^{*(n+1)} + \psi^{*(n-1)}), \Lambda^\alpha (\psi^{*(n+1)} - \psi^{*(n-1)})) = \frac{1}{4\tau} (\|\Lambda^\alpha \psi^{*(n+1)}\|^2 - \|\Lambda^\alpha \psi^{*(n-1)}\|^2); \end{aligned}$$

According to the definition of finite difference operator, we can obtain:

$$\begin{aligned} \text{Re}(\delta_t^2 \psi^{*n}, \delta_t \psi^{*n}) &= \text{Re}\left(\frac{\psi^{*(n+1)} - 2\psi^{*n} + \psi^{*(n-1)}}{\tau^2}, \frac{\psi^{*(n+1)} - \psi^{*(n-1)}}{2\tau}\right) \\ &= \frac{1}{2\tau} \text{Re}(\delta_t \psi^{*n} - \delta_t^{*(n-1)}, \delta_t \psi^{*n} + \delta_t^{*(n-1)}) = \frac{1}{2\tau} (\|\delta_t \psi^{*n}\|^2 - \|\delta_t \psi^{*(n-1)}\|^2); \end{aligned}$$

Similarly, there can also be:

$$\text{Re}(\hat{\psi}^{*n}, \delta_t \psi^{*n}) = \text{Re}\left(\frac{\psi^{*(n+1)} + \psi^{*(n-1)}}{2}, \frac{\psi^{*(n+1)} - \psi^{*(n-1)}}{2\tau}\right) = \frac{1}{4\tau} (\|\psi^{*(n+1)}\|^2 - \|\psi^{*(n-1)}\|^2);$$

Based on the previous preparation, we have

$$\begin{aligned}
 \operatorname{Im}(\delta_t^2 \psi^{*n}, \hat{\psi}^{*n}) &= \operatorname{Im}\left(\frac{\psi^{*(n+1)} - \psi^{*n}}{\tau^2} - \frac{\psi^{*n} - \psi^{*(n-1)}}{\tau^2}, \frac{\psi^{*(n+1)} + \psi^{*(n-1)}}{2}\right) \\
 &= \frac{1}{2\tau} \operatorname{Im}(\delta_t \psi^{*n} - \delta_t \psi^{*(n-1)}, \psi^{*(n+1)} + \psi^{*(n-1)}) \\
 &= \frac{1}{2\tau} \left(2\operatorname{Im}(\delta_t \psi^{*n}, \psi^{*n}) + \operatorname{Im}(\delta_t \psi^{*n}, \psi^{*(n+1)} - \psi^{*n}) - \operatorname{Im}(\delta_t \psi^{*n}, \psi^{*n} - \psi^{*(n-1)}) \right. \\
 &\quad \left. - \operatorname{Im}(\delta_t \psi^{*(n-1)}, \psi^{*(n+1)} - \psi^{*n}) - \operatorname{Im}(\delta_t \psi^{*(n-1)}, \psi^{*n} - \psi^{*(n-1)}) - 2\operatorname{Im}(\delta_t \psi^{*(n-1)}, \psi^{*(n-1)})\right) \\
 &= \frac{1}{\tau} (\operatorname{Im}(\delta_t \psi^{*n}, \psi^{*n}) - \operatorname{Im}(\delta_t \psi^{*(n-1)}, \psi^{*(n-1)})).
 \end{aligned}$$

Thus, the proof is complete. \square

Based on the above conclusion, two kinds of conservation laws are proved.

Theorem 1. The discrete scheme (12) satisfies both mass and energy conservation laws:

$$\begin{aligned}
 \text{Mass Conservation : } M^n &= M^0, \quad 0 \leq n \leq N, \\
 \text{Energy Conservation : } E^n &= E^0, \quad 0 \leq n \leq N,
 \end{aligned} \tag{21}$$

where

$$\begin{aligned}
 M^n &:= \operatorname{Im}(\delta_t \psi^{*n}, \psi^{*n}) + \frac{\gamma}{4} (\|\psi^{*(n+1)}\|^2 + \|\psi^{*n}\|^2), \\
 E^n &:= \|\delta_t \psi^{*n}\|^2 + \frac{1}{2} (\|\Lambda^\alpha \psi^{*(n+1)}\|^2 + \|\Lambda^\alpha \psi^{*n}\|^2) + \frac{\beta}{4} (\|\psi^{*(n+1)}\|_4^4 + \|\psi^{*n}\|_4^4).
 \end{aligned} \tag{22}$$

Proof. First, computing the discrete inner product of scheme (12) with $\hat{\psi}^{*n} = \frac{\psi^{*(n+1)} + \psi^{*(n-1)}}{2}$, then taking the imaginary part:

$$\operatorname{Im}\left((\delta_t^2 \psi^{*n}, \hat{\psi}^{*n}) + (\Delta_h^\alpha \hat{\psi}^{*n}, \hat{\psi}^{*n}) + (i\gamma \delta_t \psi^{*n}, \hat{\psi}^{*n}) + \left(\frac{\beta}{2} (\|\psi^{*(n+1)}\|^2 + \|\psi^{*(n-1)}\|^2) \hat{\psi}^{*n}, \hat{\psi}^{*n}\right)\right) = 0. \tag{23}$$

Combining Equation (23) with Lemma 3:

$$\frac{1}{\tau} (\operatorname{Im}(\delta_t \psi^{*n}, \psi^{*n}) - \operatorname{Im}(\delta_t \psi^{*(n-1)}, \psi^{*(n-1)})) + \frac{\gamma}{4\tau} (\|\psi^{*(n+1)}\|^2 - \|\psi^{*(n-1)}\|^2) = 0,$$

then we have:

$$\operatorname{Im}(\delta_t \psi^{*n}, \psi^{*n}) + \frac{\gamma}{4} (\|\psi^{*(n+1)}\|^2 + \|\psi^{*n}\|^2) = \operatorname{Im}(\delta_t \psi^{*(n-1)}, \psi^{*(n-1)}) + \frac{\gamma}{4} (\|\psi^{*n}\|^2 + \|\psi^{*(n-1)}\|^2),$$

which means $M^n = M^{n-1} = \dots = M^0$.

Second, computing the discrete inner product of scheme (12) with $\delta_t \psi^{*n} = \frac{\psi^{*(n+1)} - \psi^{*(n-1)}}{2\tau}$, then taking the real part,

$$\operatorname{Re}\left(\delta_t^2 \psi_j^{*n} + \Delta_h^\alpha \hat{\psi}_j^{*n} + i\gamma \delta_t \psi_j^{*n} + \frac{\beta}{2} (|\psi_j^{*(n-1)}|^2 + |\psi_j^{*(n+1)}|^2) \hat{\psi}_j^{*n}, \delta_t \psi^{*n}\right) = 0. \tag{24}$$

Combining Equation (24) with Lemma 3, we can obtain:

$$\begin{aligned}
 &\frac{1}{2\tau} (\|\delta_t \psi^{*n}\|^2 - \|\delta_t \psi^{*(n-1)}\|^2) + \frac{1}{4\tau} (\|\psi^{*(n+1)}\|^2 - \|\psi^{*(n-1)}\|^2) \\
 &\quad + \frac{\beta}{8\tau} (|\psi^{*(n+1)}|^2 + |\psi^{*(n-1)}|^2) (\|\psi^{*(n+1)}\|^2 - \|\psi^{*(n-1)}\|^2) = 0,
 \end{aligned}$$

then we have:

$$\begin{aligned} & \|\delta_t \psi^{*n}\|^2 + \frac{1}{2} (\|\Lambda^\alpha \psi^{*(n+1)}\|^2 + \|\Lambda^\alpha \psi^{*n}\|^2) + \frac{\beta}{4} (\|\psi^{*(n+1)}\|_4^4 + \|\psi^{*n}\|_4^4) \\ &= \|\delta_t \psi^{*(n-1)}\|^2 + \frac{1}{2} (\|\Lambda^\alpha \psi^{*n}\|^2 + \|\Lambda^\alpha \psi^{*(n-1)}\|^2) + \frac{\beta}{4} (\|\psi^{*n}\|_4^4 + \|\psi^{*(n-1)}\|_4^4), \end{aligned}$$

which means $E^n = E^{n-1} = \dots = E^0$.

Thus, the proof is complete. \square

5. Convergence and Stability

In this section, the proposed difference schemes (12) are proven to have second-order convergence accuracy in both space and time. To illustrate the proof, let us introduce some theorems.

Lemma 4. If $\{\Phi^n \mid n \geq 0\}$ is a non-negative sequence, then it satisfies (Gronwall inequality [32]):

$$\Phi^{n+1} \leq (1 + c\tau)\Phi^n + \tau\sigma, \quad n \geq 0, \quad (25)$$

where c and σ are non-negative constants. Φ^n satisfies

$$\Phi^{n+1} \leq e^{cn\tau} \left(\Phi^0 + \frac{\sigma}{c} \right). \quad (26)$$

Lemma 5. For any discrete functions ψ^{*n} , there holds:

$$\|\psi^{*n}\|^2 - \|\psi^{*(n+1)}\|^2 \leq \tau (\|\delta_t \psi^{*n}\|^2 + \frac{1}{2} (\|\psi^{*n}\|^2 + \|\psi^{*(n+1)}\|^2)). \quad (27)$$

For the convenience of subsequent proofs, we first proved the boundedness of numerical solutions.

Theorem 2. For $\psi^{*n} \in \mathcal{V}_h$ there exists a positive constant C , such that

$$\|\psi^{*n}\| \leq C; \quad \|\Lambda^\alpha \psi^{*n}\| \leq C; \quad \|\delta_t \psi^{*n}\| \leq C; \quad n = 0, 1, \dots, N. \quad (28)$$

Proof. Using Theorem 1 yields

$$E^n = \|\delta_t \psi^{*n}\|^2 + \frac{1}{2} (\|\Lambda^\alpha \psi^{*(n+1)}\|^2 + \|\Lambda^\alpha \psi^{*n}\|^2) + \frac{\beta}{4} (\|\psi^{*(n+1)}\|_4^4 + \|\psi^{*n}\|_4^4) = E^0,$$

and we have

$$\|\delta_t \psi^{*n}\|^2 + \frac{1}{2} (\|\Lambda^\alpha \psi^{*(n+1)}\|^2 + \|\Lambda^\alpha \psi^{*n}\|^2) = E^0 - \frac{\beta}{4} (\|\psi^{*(n+1)}\|_4^4 + \|\psi^{*n}\|_4^4).$$

Because of $\beta > 0$, it satisfies

$$\|\delta_t \psi^{*n}\|^2 + \frac{1}{2} (\|\Lambda^\alpha \psi^{*(n+1)}\|^2 + \|\Lambda^\alpha \psi^{*n}\|^2) \leq C. \quad (29)$$

Summing the inequalities (27) of Lemma 5 from 0 to n yields

$$(1 - \frac{\tau}{2}) \|\psi^{*(n+1)}\|^2 \leq (1 + \frac{\tau}{2}) \|\psi^{*0}\|^2 + \tau \|\delta_t \psi^{*0}\|^2 + \tau \sum_{k=1}^n (\|\delta_t \psi^{*k}\|^2 + \|\psi^{*k}\|^2). \quad (30)$$

Take a sum of (29) and (30) to arrive at

$$(1 - \frac{\tau}{2}) \|\psi^{*(n+1)}\|^2 + \|\delta_t \psi^{*n}\|^2 + \frac{1}{2} (\|\Lambda^\alpha \psi^{*(n+1)}\|^2 + \|\Lambda^\alpha \psi^{*n}\|^2) \leq C + \tau \sum_{k=1}^n (\|\delta_t \psi^{*k}\|^2 + \|\psi^{*k}\|^2).$$

When τ is sufficiently small ($\tau < 1$), this implies that

$$\begin{aligned} & \frac{1}{2} \|\psi^{*(n+1)}\|^2 + \|\delta_t \psi^{*n}\|^2 + \frac{1}{2} (\|\Lambda^\alpha \psi^{*(n+1)}\|^2 + \|\Lambda^\alpha \psi^{*n}\|^2) \\ & \leq C + 2\tau \sum_{k=1}^n (\frac{1}{2} \|\psi^{*k}\|^2 + \|\delta_t \psi^{*(k-1)}\|^2 + \frac{1}{2} (\|\Lambda^\alpha \psi^{*k}\|^2 + \|\Lambda^\alpha \psi^{*(k-1)}\|^2)), \end{aligned}$$

according to the discrete Gronwall's inequality [33], there is

$$\frac{1}{2} \|\psi^{*(n+1)}\|^2 + \|\delta_t \psi^{*n}\|^2 + \frac{1}{2} (\|\Lambda^\alpha \psi^{*(n+1)}\|^2 + \|\Lambda^\alpha \psi^{*n}\|^2) \leq C.$$

Thus,

$$\|\psi^{*n}\|^2 \leq C; \quad \|\Lambda^\alpha \psi^{*n}\|^2 \leq C; \quad \|\delta_t \psi^{*n}\|^2 \leq C.$$

Thus, the proof is completed. \square

Lemma 6. For any complex functions Φ, Ψ, ϕ, ψ , the following equation is satisfied (see [34])

$$|\Phi|^2 \Psi - |\phi|^2 \psi \leq (\max\{|\Phi|, |\Psi|, |\phi|, |\psi|\})^2 \cdot (2|\Phi - \phi| + |\Psi - \psi|). \quad (31)$$

Let r_j^n be the local truncation error of scheme (12). Then,

$$r_j^n = \delta_t^2 \psi_j^n + \Delta_h^\alpha \hat{\psi}_j^n + i\gamma \delta_t \psi_j^n + \frac{\beta}{2} (|\psi_j^{n-1}|^2 + |\psi_j^{n+1}|^2) \hat{\psi}_j^n. \quad (32)$$

It follows from Equation (9) and Taylor's expansion that there exists constant $C > 0$ such that

$$|r_j^n| \leq C(\tau^2 + h^2). \quad (33)$$

Theorem 3. Suppose that $\psi(x, t)$ is the solution of scheme (1). Let ψ^{*n} be the solution of the numerical scheme (12). For sufficiently small steps $\tau \lesssim h$, the schemes (12) are convergent in L^2 norm, and we have:

$$\|\epsilon^n\| = \|\psi^n - \psi^{*n}\| \lesssim \tau^2 + h^2. \quad (34)$$

Proof. Let $\epsilon_j^n = \psi_j^n - \psi_j^{*n}$, subtracting Equation (32) from Equation (12) leads to

$$r_j^n = \delta_t^2 \epsilon_j^n + \Delta_h^\alpha \hat{\epsilon}_j^n + i\gamma \delta_t \epsilon_j^n + \hat{H}_j^n, \quad (35)$$

where

$$\hat{H}_j^n = \frac{\beta}{2} (|\psi_j^{n-1}|^2 + |\psi_j^{n+1}|^2) \hat{\psi}_j^n - \frac{\beta}{2} (|\psi_j^{*(n-1)}|^2 + |\psi_j^{*(n+1)}|^2) \hat{\psi}_j^{*n}.$$

Applying Lemma 6 yields

$$\begin{aligned} |\hat{H}_j^n| &= \frac{\beta}{2} (|\psi_j^{n-1}|^2 + |\psi_j^{n+1}|^2) \hat{\psi}_j^n - \frac{\beta}{2} (|\psi_j^{*(n-1)}|^2 + |\psi_j^{*(n+1)}|^2) \hat{\psi}_j^{*n} \\ &= \frac{\beta}{2} |(\bar{\psi}_j^{*(n-1)} \hat{\psi}_j^{*n} \epsilon_j^{n-1} + \psi_j^{n-1} \hat{\psi}_j^{*n} \bar{\epsilon}_j^{n-1} + |\psi_j^{n-1}|^2 \hat{\epsilon}_j^n) \\ &\quad + (\bar{\psi}_j^{*(n+1)} \hat{\psi}_j^{*n} \epsilon_j^{n+1} + \psi_j^{n+1} \hat{\psi}_j^{*n} \bar{\epsilon}_j^{n+1} + |\psi_j^{n+1}|^2 \hat{\epsilon}_j^n)| \\ &\leq \frac{\beta}{2} (\max|\psi_j^n|, |\psi_j^{*n}|, |\psi_j^{n+1}|, |\psi_j^{*(n+1)}|)^2 (2|\epsilon_j^{n-1}| + 2|\epsilon_j^{n+1}| + 2|\hat{\epsilon}_j^n|). \end{aligned} \quad (36)$$

Thanks to Theorem 2, we derive

$$|\hat{H}_j^n|^2 \leq C(|\epsilon_j^{n-1}|^2 + |\epsilon_j^{n+1}|^2),$$

and thus,

$$\|\hat{H}_j^n\|^2 = \int_{\Omega} |\hat{H}_j^n|^2 dx \leq C(\|\epsilon_j^{n-1}\|^2 + \|\epsilon_j^{n+1}\|^2). \quad (37)$$

Computing the inner product of Equation (35) with $\delta_t \epsilon_j^n$ and then taking the real part results in:

$$\operatorname{Re}(r_j^n, \delta_t \epsilon_j^n) = \operatorname{Re}(\delta_t^2 \epsilon_j^n, \delta_t \epsilon_j^n) + \operatorname{Re}(\Delta_h^\alpha \hat{\epsilon}_j^n, \delta_t \epsilon_j^n) + \operatorname{Re}(i\gamma \delta_t \epsilon_j^n, \delta_t \epsilon_j^n) + \operatorname{Re}(\hat{H}_j^n, \delta_t \epsilon_j^n).$$

Lemma 3 yields:

$$\operatorname{Re}(r_j^n, \delta_t \epsilon_j^n) = \frac{1}{2\tau}(\|\delta_t \epsilon_j^n\|^2 - \|\delta_t \epsilon_j^{n-1}\|^2) + \frac{1}{4\tau}(\|\Lambda^\alpha \epsilon_j^{n+1}\|^2 - \|\Lambda^\alpha \epsilon_j^{n-1}\|^2) + \operatorname{Re}(\hat{H}_j^n, \delta_t \epsilon_j^n).$$

That is:

$$\frac{1}{2\tau}(\|\delta_t \epsilon_j^n\|^2 - \|\delta_t \epsilon_j^{n-1}\|^2) + \frac{1}{4\tau}(\|\Lambda^\alpha \epsilon_j^{n+1}\|^2 - \|\Lambda^\alpha \epsilon_j^{n-1}\|^2) = \operatorname{Re}(r_j^n, \delta_t \epsilon_j^n) - \operatorname{Re}(\hat{H}_j^n, \delta_t \epsilon_j^n). \quad (38)$$

Moreover,

$$\begin{aligned} \operatorname{Re}(r_j^n, \delta_t \epsilon_j^n) &= \frac{1}{2} \operatorname{Re}(r_j^n, \delta_t \epsilon_j^n + \delta_t \epsilon_j^{n-1}) \leq \frac{1}{2} \|r_j^n\|^2 \|\delta_t \epsilon_j^n + \delta_t \epsilon_j^{n-1}\|^2 \\ &\leq \frac{1}{2} (\|r_j^n\|^2 + \frac{1}{4} \|\delta_t \epsilon_j^n + \delta_t \epsilon_j^{n-1}\|^2) \\ &\leq \frac{1}{2} (\|r_j^n\|^2 + \|\delta_t \epsilon_j^n\|^2 + \|\delta_t \epsilon_j^{n-1}\|^2). \end{aligned} \quad (39)$$

Similarly, Equation (37) yields

$$\begin{aligned} \operatorname{Re}(\hat{H}_j^n, \delta_t \epsilon_j^n) &\leq C(\|\hat{H}_j^n\|^2 + \|\delta_t \epsilon_j^n\|^2 + \|\delta_t \epsilon_j^{n-1}\|^2) \\ &\leq C(\|\epsilon_j^{n+1}\|^2 + \|\epsilon_j^{n-1}\|^2 + \|\delta_t \epsilon_j^n\|^2 + \|\delta_t \epsilon_j^{n-1}\|^2). \end{aligned} \quad (40)$$

From Lemma 5,

$$\|\epsilon_j^n\|^2 - \|\epsilon_j^{n-1}\|^2 \leq \tau(\|\delta_t \epsilon_j^{n-1}\|^2 + \frac{1}{2}(\|\epsilon_j^n\|^2 + \|\epsilon_j^{n-1}\|^2)). \quad (41)$$

Substituting Equations (39) and (40) into Equation (38) and using Equations (41) and (33) leads to

$$\begin{aligned} &\frac{1}{2\tau}(\|\delta_t \epsilon_j^n\|^2 - \|\delta_t \epsilon_j^{n-1}\|^2) + \frac{1}{4\tau}(\|\Lambda^\alpha \epsilon_j^{n+1}\|^2 - \|\Lambda^\alpha \epsilon_j^{n-1}\|^2) + \frac{1}{\tau}(\|\epsilon_j^n\|^2 - \|\epsilon_j^{n-1}\|^2) \\ &\leq C((\|\epsilon_j^{n-1}\|^2 + \|\epsilon_j^n\|^2 + \|\epsilon_j^{n+1}\|^2 + \|\delta_t \epsilon_j^n\|^2 + \|\delta_t \epsilon_j^{n-1}\|^2 + (\tau^2 + h^2)^2)). \end{aligned} \quad (42)$$

The purpose of this step is to bound the growth of the error by terms of the order of the truncation error and the errors at previous time levels. The inequalities (39) and (40) are used to control the inner products involving r_j^n and \hat{H}_j^n , while (41) is used to handle the L^2 -norm of the error itself. Then,

$$\begin{aligned} &(\frac{1}{2} \|\delta_t \epsilon_j^n\|^2 + \frac{1}{4} (\|\Lambda^\alpha \epsilon_j^{n+1}\|^2 + \|\Lambda^\alpha \epsilon_j^n\|^2) + \|\epsilon_j^n\|^2) - \\ &(\frac{1}{2} \|\delta_t \epsilon_j^{n-1}\|^2 + \frac{1}{4} (\|\Lambda^\alpha \epsilon_j^n\|^2 + \|\Lambda^\alpha \epsilon_j^{n-1}\|^2) + \|\epsilon_j^{n-1}\|^2) \\ &\leq \tau C((\|\epsilon_j^{n-1}\|^2 + \|\epsilon_j^n\|^2 + \|\epsilon_j^{n+1}\|^2 + \|\delta_t \epsilon_j^n\|^2 + \|\delta_t \epsilon_j^{n-1}\|^2 + (\tau^2 + h^2)^2)). \end{aligned} \quad (43)$$

Thus, taking the sum of (43) from 1 to n , we have

$$\begin{aligned} & \frac{1}{2} \|\delta_t \epsilon_j^n\|^2 + \frac{1}{4} (\|\Lambda^\alpha \epsilon_j^{n+1}\|^2 + \|\Lambda^\alpha \epsilon_j^n\|^2) + \|\epsilon_j^n\|^2 \\ & \leq \tau C \sum_{i=1}^n \left(\frac{1}{2} \|\delta_t \epsilon_j^i\|^2 + \frac{1}{4} (\|\Lambda^\alpha \epsilon_j^{i+1}\|^2 + \|\Lambda^\alpha \epsilon_j^i\|^2) + \|\epsilon_j^i\|^2 \right) + C(\tau^2 + h^2)^2. \end{aligned} \quad (44)$$

The resulting inequality (44) is now in a form where the discrete Gronwall inequality (Lemma 4) can be applied to bound the cumulative error growth over all time steps.

Hence, using the discrete Gronwall's inequality gives

$$\frac{1}{2} \|\delta_t \epsilon_j^n\|^2 + \frac{1}{4} (\|\Lambda^\alpha \epsilon_j^{n+1}\|^2 + \|\Lambda^\alpha \epsilon_j^n\|^2) + \|\epsilon_j^n\|^2 \leq C(\tau^2 + h^2)^2. \quad (45)$$

Thus,

$$\|\epsilon_j^n\|^2 \leq C(\tau^2 + h^2)^2. \quad (46)$$

Then, we have

$$\|\epsilon_j^n\| \leq C(\tau^2 + h^2). \quad (47)$$

This completes the proof. \square

Theorem 4. Under the conditions of the Theorem 3, the solution of the scheme (12) is unconditionally stable with respect to initial values in the discrete l^2 -norm.

6. Numerical Examples

In this section, we use the proposed implicit difference scheme (12) to solve practical problem to verify its effectiveness. The L^2 - norm sense is defined as

$$L^2 \text{ error} = \sqrt{h \sum_j |\psi_j^k - \psi^*(x_j[a-z]_k)|^2}, \quad (48)$$

then the convergence rates in time and space in the L^2 - norm follow the following formula [35]:

$$\text{Rate} = \begin{cases} \frac{\log(\|e(\tau_1, N)\| / \|e(\tau_2, N)\|)}{\log(\tau_1 / \tau_2)} & \text{in time,} \\ \frac{\log(\|e(\tau, N_1)\| / \|e(\tau, N_2)\|)}{\log(N_1 / N_2)} & \text{in space.} \end{cases} \quad (49)$$

The relative errors of energy and mass are defined as

$$RM^n = |(M^n - M^0) / M^0|, \quad RE^n = |(E^n - E^0) / E^0|, \quad (50)$$

Example 1. The following nonlinear space-fractional Schrödinger Equation [36] with wave operator is considered.

$$\psi_{tt}(x, t) + (-\Delta)^{\alpha/2} \psi(x, t) + i\psi_t(x, t) + |\psi(x, t)|^2 \psi(x, t) = 0, \quad x \in (a, b), t \in (0, T], \quad (51)$$

with the following initial condition:

$$\psi(x, 0) = (1 + i)x \cdot \exp(-10(1 - x)^2), \quad \psi_t(x, 0) = 0.$$

When $\alpha = 2$, the analytical solution of Equation (51) is:=

$$\psi(x, t) = \text{sech}(x - 4t) \cdot \exp(i(2x - 3t)).$$

We take $(a, b) = (-25, 25)$, $t \in (0, 10]$, and we set $\psi(a, t) = \psi(b, t) = 0$. Figures 1–4 show the image of the numerical solution when $\alpha = 1.1, 1.4, 1.7$, and 2, respectively. As shown in the figure, the value of fractional order α affects the shape contour of the numerical solution. The smaller the value of the fractional order, the faster the shape of the numerical solution changes, and the larger the value, the flatter the image of the numerical solution, similar to the situation of integer order. Figure 1 shows the evolution of the wave function for $\alpha = 1.1$. The sub-diffusive nature of the fractional derivative ($\alpha = 1.1$) leads to a slower spread and a more pronounced peak of the wave packet compared to the classical case ($\alpha = 2$, Figure 4), illustrating the impact of long-range interactions and anomalous diffusion on quantum wave propagation. Physically, using this characteristic, the fractional order Schrödinger equation can be used to correct waveforms without changing nonlinearity and dispersion effects.

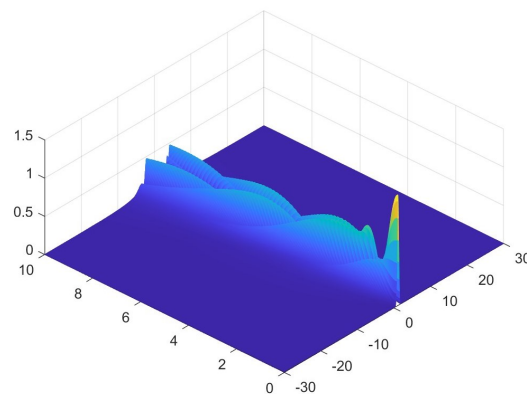


Figure 1. Numerical solution for $\alpha = 1.1$.

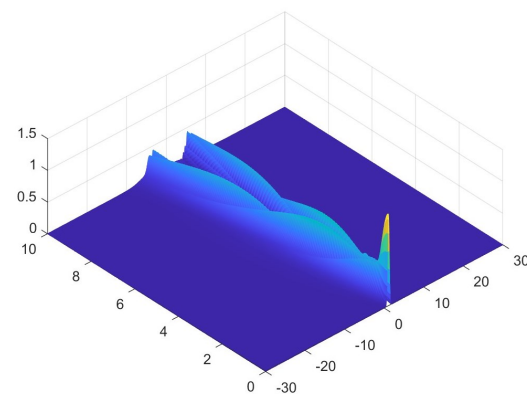


Figure 2. Numerical solution for $\alpha = 1.4$.

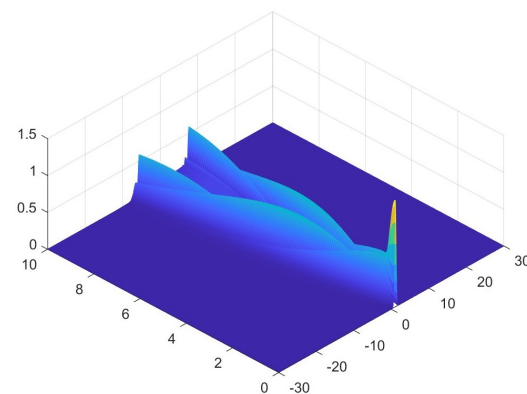


Figure 3. Numerical solution for $\alpha = 1.7$.

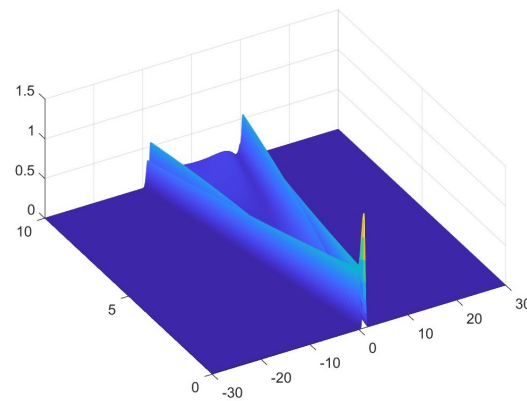


Figure 4. Numerical solution for $\alpha = 2$.

We calculated the discrete conservation law. Figure 5 (Left) shows the evolution of the discrete mass. The overlapping curves for different α values confirm that the mass conservation law holds exactly for our numerical scheme, independent of the fractional order. This is a critical property for simulating closed quantum systems. Figure 5 (Right) displays the corresponding relative error, which remains at the level of machine precision, numerically verifying the conservation property. Figure 6 (Left) depicts the evolution of the discrete energy. The energy remains constant over time, confirming the energy-conserving property of the scheme. The value of the conserved energy depends on α as the fractional Laplacian operator itself is α -dependent. Figure 6 (Right) reveals the corresponding relative error, which remains very small, demonstrating the scheme's ability to preserve energy over long-term simulations.

We established a fixed spatial step, and Table 1 presents the temporal error along with the convergence order at $T = 1$. The convergence sequence demonstrates that our scheme achieves second-order accuracy in time. Subsequently, we maintained a constant time step $\tau = 0.001$ to evaluate the spatial error of the proposed method. The spatial errors for the nonlinear fractional Schrödinger equation across various values of α are illustrated in Table 2, indicating that our difference scheme also attains second-order accuracy in space.

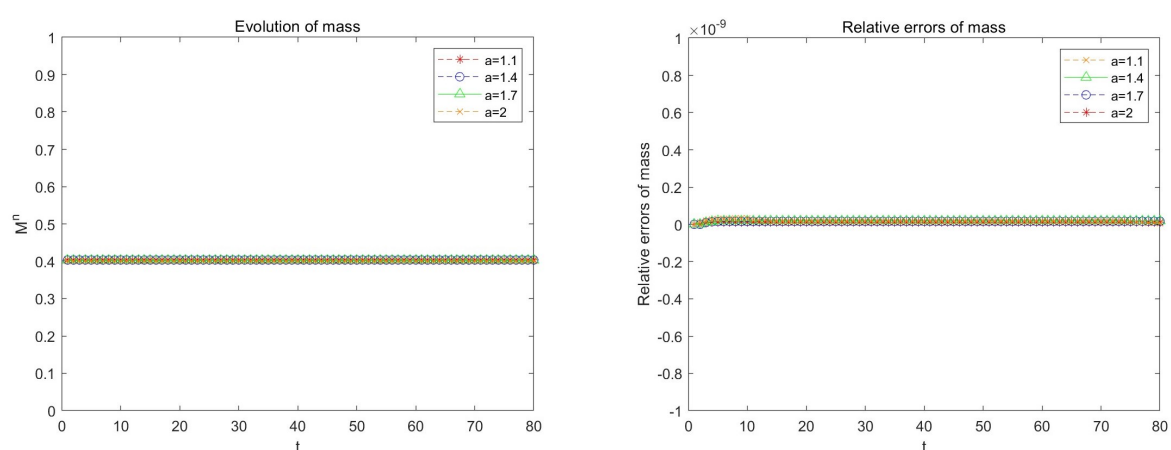


Figure 5. The conservation of M^n and the error function RM^n with different α values. **Left:** the four curves overlap with each other.

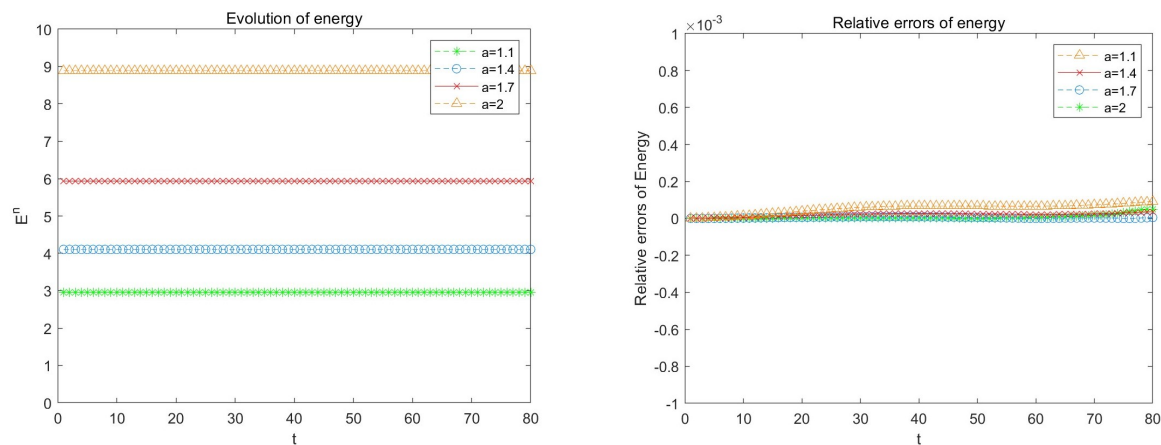


Figure 6. The conservation of E^n and the error function RE^n with different α values.

Table 1. Errors and convergence orders of scheme (12) for Equation (51) at time $t = 1$ with $M = 4000$.

τ	$\alpha = 1.1$		$\alpha = 1.4$		$\alpha = 1.7$		$\alpha = 2$	
	Error	Rate	Error	Rate	Error	Rate	Error	Rate
0.2	7.69×10^{-1}		1.04		1.41		1.89	
0.1	2.15×10^{-1}	1.84	3.06×10^{-1}	1.76	4.56×10^{-1}	1.64	6.85×10^{-1}	1.46
0.05	5.29×10^{-2}	2.02	7.69×10^{-2}	1.99	1.19×10^{-1}	1.94	1.90×10^{-1}	1.85
0.025	1.07×10^{-2}	2.31	1.56×10^{-2}	2.30	2.43×10^{-2}	2.29	3.98×10^{-2}	2.25

Table 2. Errors and convergence orders of scheme (12) for Equation (51) at time $t = 1$ with $\tau = 0.01$.

h	$\alpha = 1.1$		$\alpha = 1.4$		$\alpha = 1.7$		$\alpha = 2$	
	Error	Rate	Error	Rate	Error	Rate	Error	Rate
0.2	1.17		7.86×10^{-1}		6.75×10^{-1}		4.64×10^{-1}	
0.1	3.29×10^{-1}	1.83	2.29×10^{-1}	1.78	1.83×10^{-1}	1.88	1.23×10^{-1}	1.91
0.05	7.88×10^{-2}	2.06	5.95×10^{-2}	1.95	4.75×10^{-2}	1.95	2.95×10^{-2}	2.06
0.025	1.96×10^{-2}	2.01	1.46×10^{-2}	2.02	1.22×10^{-2}	1.96	7.24×10^{-3}	2.03

Example 2. The nonlinear space-fractional Schrödinger equation [37] is considered:

$$\psi_{tt}(x, t) + (-\Delta)^{\alpha/2} \psi(x, t) + i\psi_t(x, t) + |\psi(x, t)|^2 \psi(x, t) = 0, \quad x \in (-25, 25), t \in (0, 10], \quad (52)$$

with the following initial conditions:

$$\psi(x, 0) = \text{sech}(x) \exp(4ix), \quad \psi_t(x, 0) = -\text{sech}(x) \tanh(x) \exp(4ix).$$

Figures 7–10 show the images of numerical solutions when $\alpha = 1.1, 1.4, 1.7$, and 2 , respectively. Because the equation does not have an exact solution, for the convenience of comparison, the numerical solution of the finite difference method with smaller time and space steps is taken as the exact solution. When α approaches 2 , the numerical solution of the fractional order equation converges to the solution of the classical non-fractional order equation.

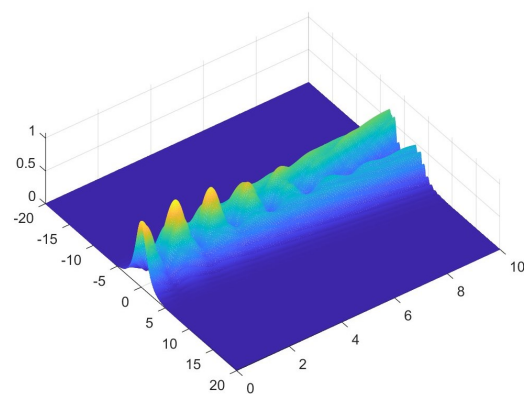


Figure 7. Numerical solution for $\alpha = 1.1$.

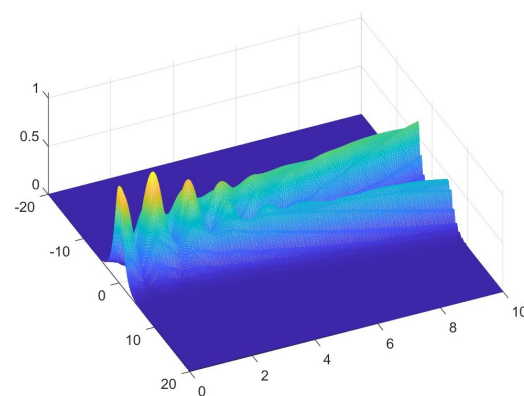


Figure 8. Numerical solution for $\alpha = 1.4$.

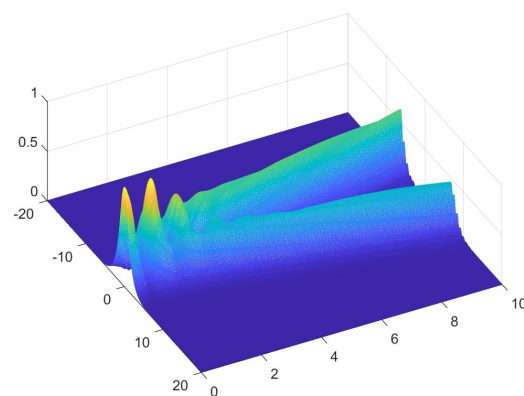


Figure 9. Numerical solution for $\alpha = 1.7$.

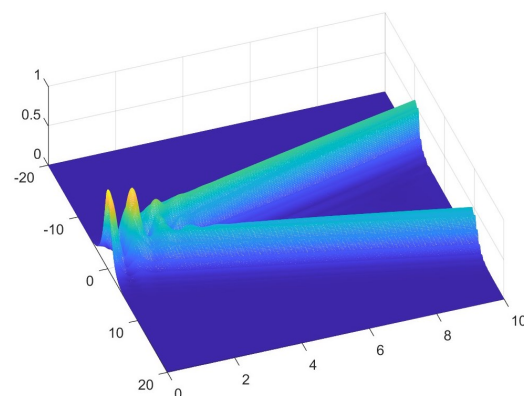


Figure 10. Numerical solution for $\alpha = 2$.

Figure 11 depicts the evolution of mass and relative errors of mass, and Figure 12 depicts the evolution of energy and relative errors of energy. The results indicate that the schemes effectively maintain the conservation of mass and energy, and the energy varies with the change in α value. However, the mass conservation is independent of α . Therefore, the four curves in the left figure of Figure 5 overlap with each other.

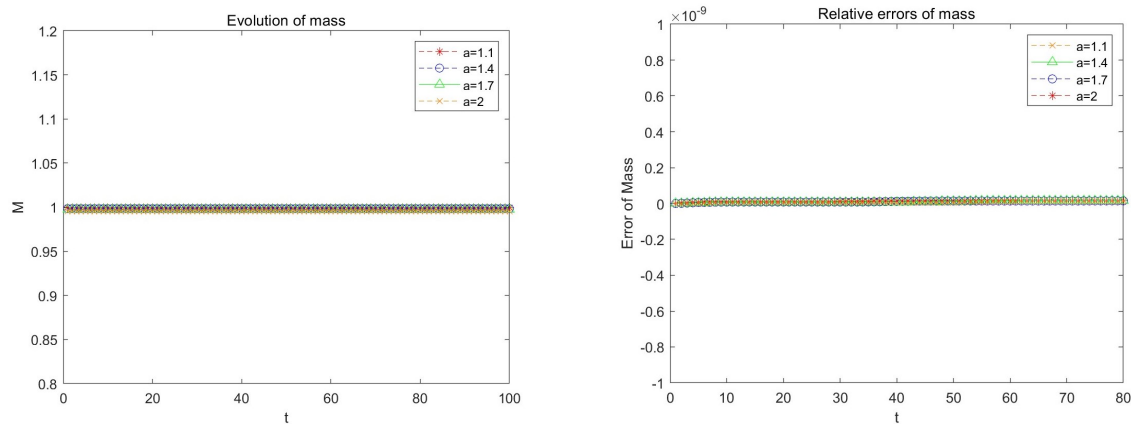


Figure 11. The conservation of M^n and the error function RM^n with different α values. **Left:** the four curves overlap with each other.

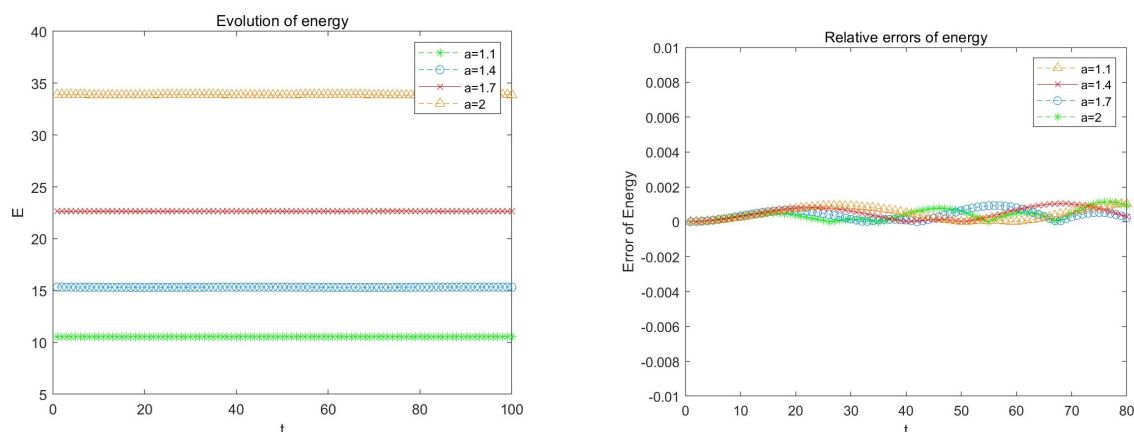


Figure 12. The conservation of E^n and the error function RE^n with different α values.

We established a fixed spatial step, and Table 3 presents the temporal error along with the convergence order at $T = 1$. The convergence sequence demonstrates that our scheme achieves second-order accuracy in time. Subsequently, we maintained a constant time step $\tau = 0.001$ to evaluate the spatial error of the proposed method. The spatial errors for the nonlinear fractional Schrödinger equation across various values of α are illustrated in Table 4, indicating that our difference scheme also attains second-order accuracy in space.

Table 3. Errors and convergence orders of scheme (12) for Equation (52) at time $t = 1$ with $M = 4000$.

τ	$\alpha = 1.1$		$\alpha = 1.4$		$\alpha = 1.7$		$\alpha = 2$	
	Error	Rate	Error	Rate	Error	Rate	Error	Rate
0.1	3.50×10^{-1}		5.31×10^{-1}		7.75×10^{-1}		8.45×10^{-1}	
0.05	9.92×10^{-2}	1.82	1.52×10^{-1}	1.80	2.22×10^{-1}	1.80	2.20×10^{-1}	1.94
0.025	2.57×10^{-2}	1.95	3.65×10^{-2}	2.06	5.79×10^{-2}	1.94	5.64×10^{-2}	1.97
0.0125	6.23×10^{-3}	2.05	8.45×10^{-3}	2.11	1.45×10^{-2}	2.00	1.23×10^{-2}	2.20

Table 4. Errors and convergence orders of scheme (12) for Equation (52) at time $t = 1$ with $\tau = 0.01$.

h	$\alpha = 1.1$		$\alpha = 1.4$		$\alpha = 1.7$		$\alpha = 2$	
	Error	Rate	Error	Rate	Error	Rate	Error	Rate
0.1	3.07×10^{-3}		9.77×10^{-4}		9.92×10^{-4}		6.43×10^{-3}	
0.05	8.30×10^{-4}	1.89	2.47×10^{-4}	1.99	2.49×10^{-4}	2.00	1.62×10^{-3}	1.99
0.025	2.16×10^{-4}	1.94	5.97×10^{-5}	2.05	5.71×10^{-5}	2.12	4.18×10^{-4}	1.95
0.0125	5.36×10^{-5}	2.01	1.42×10^{-5}	2.07	1.14×10^{-5}	2.33	8.44×10^{-5}	2.31

Example 3. Nonlinear space-fractional Schrödinger equation is considered:

$$\psi_{tt}(x, t) + (-\Delta)^{\alpha/2} \psi(x, t) + i\psi_t(x, t) + |\psi(x, t)|^2 \psi(x, t) = f(x, t), \quad x \in (0, 1), t \in [0, 1], \quad (53)$$

with fractional boundary conditions:

$$\frac{\partial^{\alpha-1} \psi(x, t)}{\partial |x|^{\alpha-1}} \Big|_{x=1} = \frac{1}{2}(t+1)^3 \sec\left(\frac{(\alpha-1)\pi}{2}\right) \left(\frac{\Gamma(5)}{\Gamma(6-\alpha)} - \frac{4\Gamma(6)}{\Gamma(7-\alpha)} + \frac{6\Gamma(7)}{\Gamma(8-\alpha)} - \frac{4\Gamma(8)}{\Gamma(9-\alpha)} + \frac{\Gamma(9)}{\Gamma(10-\alpha)} \right),$$

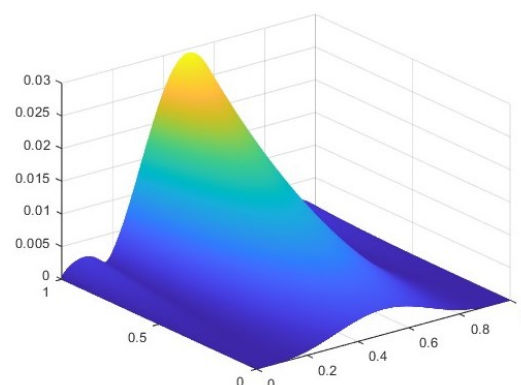
initial condition:

$$\psi(x, 0) = x^4(1-x)^4, \quad \psi_t(x, 0) = 3x^4(1-x)^4,$$

and the non-homogeneous part:

$$\begin{aligned} f(x, t) = & 6(t+1)x^4(1-x)^4 + \frac{1}{2}(t+1)^3 \sec\left(\frac{\pi\alpha}{2}\right) \left\{ \frac{\Gamma(5)}{\Gamma(5-\alpha)} [x^{4-\alpha} + (1-x)^{4-\alpha}] \right. \\ & - \frac{4\Gamma(6)}{\Gamma(6-\alpha)} [x^{5-\alpha} + (1-x)^{5-\alpha}] + \frac{6\Gamma(7)}{\Gamma(7-\alpha)} [x^{6-\alpha} + (1-x)^{6-\alpha}] \\ & - \frac{4\Gamma(8)}{\Gamma(8-\alpha)} [x^{7-\alpha} + (1-x)^{7-\alpha}] + \frac{\Gamma(9)}{\Gamma(9-\alpha)} [x^{8-\alpha} + (1-x)^{8-\alpha}] \Big\} \\ & + 3i(t+1)^2 x^4(1-x)^4 + [(t+1)^3 x^4(1-x)^4]^3. \end{aligned}$$

Figures 13–16 show the cases when $\alpha = 1.1, 1.4, 1.7$, and 2 , respectively, the image of numerical solution. When α approaches 2 , the numerical solution of the fractional order equation converges to the solution of the classical non-fractional order equation.

**Figure 13.** Numerical solution for $\alpha = 1.1$.

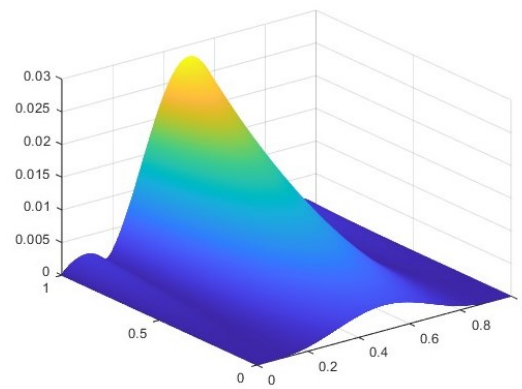


Figure 14. Numerical solution for $\alpha = 1.4$.

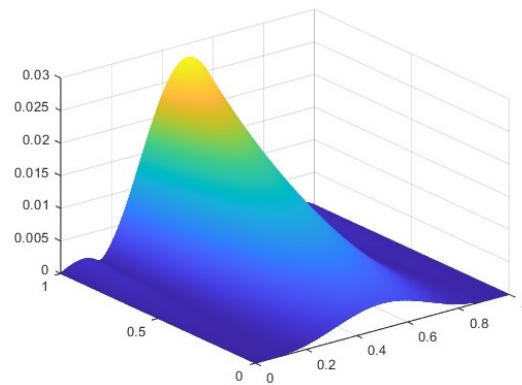


Figure 15. Numerical solution for $\alpha = 1.7$.

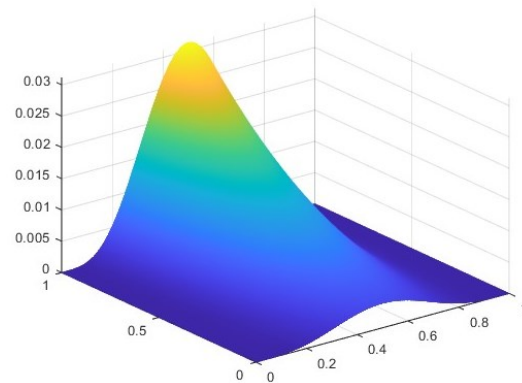


Figure 16. Numerical solution for $\alpha = 2$.

We established a fixed spatial step, and Table 5 presents the temporal error along with the convergence order at $T = 1$. The convergence sequence demonstrates that our scheme achieves second-order accuracy in time. Subsequently, we maintained a constant time step $\tau = 0.005$ to evaluate the spatial error of the proposed method. The spatial errors for the nonlinear fractional Schrödinger equation across various values of α are illustrated in Table 6, indicating that our difference scheme also attains second-order accuracy in space. In this place, we are still ready to discuss the conservation of energy and mass, but this equation no longer satisfies the conservation property due to the source term $f(x, t)$ not being equivalent to zero.

Table 5. Errors and convergence orders of scheme (12) for Equation (53) at time $t = 1$ with $M = 1000$.

τ	$\alpha = 1.1$		$\alpha = 1.4$		$\alpha = 1.7$		$\alpha = 2$	
	Error	Rate	Error	Rate	Error	Rate	Error	Rate
0.1	7.52×10^{-4}		1.07×10^{-3}		1.12×10^{-3}		2.85×10^{-4}	
0.05	1.80×10^{-4}	2.07	2.60×10^{-4}	2.04	2.73×10^{-4}	2.03	6.89×10^{-5}	2.05
0.025	4.40×10^{-5}	2.03	6.45×10^{-5}	2.01	6.80×10^{-5}	2.01	1.60×10^{-5}	2.11
0.0125	1.09×10^{-5}	2.01	1.60×10^{-5}	2.01	1.70×10^{-5}	2.00	3.99×10^{-6}	2.00

Table 6. Errors and convergence orders of scheme (12) for Equation (53) at time $t = 1$ with $\tau = 0.005$.

h	$\alpha = 1.1$		$\alpha = 1.4$		$\alpha = 1.7$		$\alpha = 2$	
	Error	Rate	Error	Rate	Error	Rate	Error	Rate
0.1	1.35×10^{-3}		4.40×10^{-3}		3.92×10^{-3}		5.53×10^{-3}	
0.05	3.08×10^{-4}	2.14	1.01×10^{-3}	2.13	9.34×10^{-4}	2.07	1.29×10^{-3}	2.09
0.025	6.97×10^{-5}	2.14	2.24×10^{-4}	2.17	2.16×10^{-4}	2.11	3.13×10^{-4}	2.05
0.0125	1.64×10^{-5}	2.09	5.32×10^{-5}	2.07	4.96×10^{-5}	2.13	6.99×10^{-5}	2.16

7. Conclusions

In this paper, a conservative difference scheme is constructed for the nonlinear spatial fractional Schrödinger equation with wave operators. For the spatial Riesz-fractional derivative, the Crank–Nicolson method is used for discretization; for the time derivative, the central difference is used for separation. Based on this difference scheme, the energy and mass conservation formulas under discrete conditions are derived and prove that the solution is unconditionally stable in this difference method. Using the energy method, this differential format has been proven to maintain second-order convergence in both time and space. Finally, through several numerical examples, the accuracy of the scheme and the effectiveness of discrete conservation law and long-term simulation are verified.

Future work will include a detailed comparative analysis of the computational efficiency of the proposed scheme against other existing methods, leveraging the structure of the linear systems for optimal performance and investigating advanced preconditioning techniques.

Author Contributions: Conceptualization, M.Z.; Methodology, C.L.; Formal analysis, M.Z. and X.Z.; Investigation, M.Z.; Writing—original draft, M.Z.; Writing—review and editing, X.Z. and C.L.; Visualization, M.Z. and X.Z.; Supervision, C.L.; Project administration, C.L.; Funding acquisition, C.L. All authors have read and agreed to the published version of the manuscript.

Funding: This document is the result of the research project funded by the National Natural Science Foundation of China under Grant No. 62373165.

Data Availability Statement: The original contributions presented in this study are included in the article. Further inquiries can be directed to the corresponding author(s).

Conflicts of Interest: The authors declare no conflicts of interest.

References

1. Zhang, X.; Yang, B.; Wei, C.Z.; Luo, M.K. Quantization method and Schrödinger equation of fractional time and their weak effects on Hamiltonian: Phase transitions of energy and wave functions. *Commun. Nonlinear Sci. Numer. Simul.* **2021**, *93*, 105531. [\[CrossRef\]](#)
2. Deng, Y.B.; Liu, C.C.; Yang, X. Standing waves of fractional Schrödinger equations with critical nonlinearities and decaying potentials. *Discret. Contin. Dyn. Syst.* **2025**, *45*, 1248–1296. [\[CrossRef\]](#)

3. Hu, D.D.; Hui, H.L.; Xu, Z.Z.; Wang, Y.S. On convergence of a novel linear conservative scheme for the two-dimensional fractional nonlinear Schrödinger equation with wave operator. *Comput. Math. Appl. Int. J.* **2023**, *150*, 254–266. [\[CrossRef\]](#)
4. Faridi, W.A.; Asjad, M.I.; Jhangeer, A.; Yusuf, A.; Sulaiman, T.A. The weakly non-linear waves propagation for Kelvin–Helmholtz instability in the magnetohydrodynamics flow impelled by fractional theory. *Opt. Quantum Electron.* **2023**, *55*, 172. [\[CrossRef\]](#)
5. Lashkarian, E.; Motamednezhad, A.; Hejazi, S.R. Invariance properties and conservation laws of perturbed fractional wave equation. *Eur. Phys. J. Plus* **2021**, *136*, 615. [\[CrossRef\]](#)
6. Zhong, M.; Yan, Z.Y. Data-driven soliton mappings for integrable fractional nonlinear wave equations via deep learning with Fourier neural operator. *Chaos Solitons Fractals* **2022**, *165*, 112787. [\[CrossRef\]](#)
7. Mohammad, M.; Sajjad, H.M.; Arzu, A.; Hamood, U.R.; Ifrah, I.; Mostafa, E. Dynamics of optical solitons in the extended(3+1)-dimensional nonlinear conformable Kudryashov equation with generalized anti-cubic nonlinearity. *Math. Methods Appl. Sci.* **2024**, *47*, 5355–5375.
8. He, X.M.; Zou, W.M. Existence and concentration result for the fractional Schrödinger equations with critical nonlinearities. *Calc. Var. Part. Differ. Equ.* **2016**, *55*, 91. [\[CrossRef\]](#)
9. Yan, J.Y.; Zhang, H.; Wei, Y.B.; Qian, X. High-order and mass-conservative regularized implicit-explicit relaxation Runge-Kutta methods for the low regularity Schrödinger equations. *Appl. Numer. Math.* **2025**, *216*, 210–221. [\[CrossRef\]](#)
10. Wang, L.L.; Yan, J.Y.; Zhang, X.L. Error analysis of a first-order IMEX scheme for the logarithmic Schrödinger equation. *SIAM J. Numer. Anal.* **2024**, *62*, 119–137. [\[CrossRef\]](#)
11. Deepika, R.; Muthunagai, K. A Novel Fractional Uncertainty Relation in Quaternionic Quantum Mechanics. *Math. Methods Appl. Sci.* **2025**, *13*, 12813–12818. [\[CrossRef\]](#)
12. Varão, G.; Lobo, I.P.; Bezerra, V.B. Fractional quantum mechanics meets quantum gravity phenomenology. *Europhys. Lett.* **2024**, *3*, 30001. [\[CrossRef\]](#)
13. Zhang, X.; Ran, M.H.; Liu, Y.; Zhang, L. A high-order structure-preserving difference scheme for generalized fractional Schrödinger equation with wave operator. *Math. Comput. Simul.* **2023**, *210*, 532–546. [\[CrossRef\]](#)
14. Yang, Q.; Liu, F.; Turner, I. Numerical methods for fractional partial differential equations with Riesz space fractional derivatives. *Appl. Math. Model.* **2010**, *34*, 200–218. [\[CrossRef\]](#)
15. Caffarelli, L. Non-local diffusions, drifts and games. In *Nonlinear Partial Differential Equations. Abel Symposium*; Springer: Berlin/Heidelberg, Germany, 2012; Volume 7, pp. 37–52.
16. Lischke, A.; Pang, G.; Gulian, M.; Song, F.; Glusa, C.; Zheng, X.; Mao, Z.; Cai, W.; Meerschaert, M.M.; Ainsworth, M.; et al. What is the fractional Laplacian? A comparative review with new results. *Comput. Phys.* **2020**, *404*, 109009. [\[CrossRef\]](#)
17. D’Elia, M.; Du, Q.; Glusa, C.; Gunzburger, M.; Tian, X.; Zhou, Z. Numerical methods for nonlocal and fractional models. *Acta Numer.* **2020**, *29*, 1–124. [\[CrossRef\]](#)
18. Bao, W.Z.; Cai, Y.Y. Uniform Error Estimates of Finite Difference Methods for the Nonlinear Schrödinger Equation with Wave Operator. *SIAM J. Numer. Anal.* **2012**, *20*, 492–521. [\[CrossRef\]](#)
19. Wang, P.D.; Huang, C.M. An energy conservative difference scheme for the nonlinear fractional Schrödinger equations. *J. Comput. Phys.* **2015**, *293*, 238–251. [\[CrossRef\]](#)
20. Yao, L.; Lei, S.L.; Sun, H.W. Efficient finite difference scheme for a hidden-memory variable-order time-fractional diffusion equation. *Comput. Appl. Math.* **2023**, *42*, 362.
21. Li, M.; Huang, C.M.; Wang, P.D. Galerkin finite element method for nonlinear fractional Schrödinger equations. *Numer. Algorithms* **2017**, *74*, 499–525. [\[CrossRef\]](#)
22. Li, M.; Gu, X.M.; Huang, C.M.; Fei, M.F.; Zhang, G.Y. A fast linearized conservative finite element method for the strongly coupled nonlinear fractional Schrödinger equations. *J. Comput. Phys.* **2018**, *258*, 256–282. [\[CrossRef\]](#)
23. Liang, X.; Khaliq, A.Q.M. An efficient Fourier spectral exponential time differencing method for the space-fractional nonlinear Schrödinger equations. *Comput. Math. Appl.* **2018**, *75*, 4438–4457. [\[CrossRef\]](#)
24. Hui, Z.; Yun, X.J.; Chu, W.; Zhen, S.C. Crank-Nicolson Fourier spectral methods for the space fractional nonlinear Schrödinger equation and its parameter estimation. *Int. J. Comput. Math.* **2019**, *96*, 238–263.
25. Bian, R.C.; Hua, Z.G. Regularized splitting spectral method for space-fractional logarithmic Schrödinger equation. *Appl. Numer. Math.* **2021**, *167*, 330–355. [\[CrossRef\]](#)
26. Amore, P.; Fernandez, F.M.; Hofmann, C.P.; Saenz, R.A. Collocation method for fractional quantum mechanics. *J. Math. Phys.* **2010**, *51*, 122101. [\[CrossRef\]](#)
27. Yan, C.; Chen, H.Z. Fourth-order finite difference scheme and efficient algorithm for nonlinear fractional Schrödinger equations. *Adv. Differ. Equ.* **2020**, *2020*, 4.
28. Wang, J.J. High-order conservative schemes for the space fractional nonlinear Schrödinger equation. *Appl. Numer. Math.* **2021**, *165*, 248–269. [\[CrossRef\]](#)
29. Li, X.X.; Wen, J.M.; Li, D.F. Mass- and energy-conserving difference schemes for nonlinear fractional Schrödinger equations. *Math. Lett.* **2021**, *111*, 106686. [\[CrossRef\]](#)

30. Çelik, C.; Duman, M. Crank-Nicolson method for the fractional diffusion equation with the Riesz fractional derivative. *J. Comput. Phys.* **2012**, *231*, 1743–1750. [[CrossRef](#)]
31. Bao, W.Z.; Cai, Y. Optimal error estimates of finite difference methods for the gross-pitaevskii equation with angular momentum rotation. *Math. Comput.* **2013**, *82*, 99–128. [[CrossRef](#)]
32. Ye, H.P.; Gao, J.M.; Ding, Y.S. A generalized Gronwall inequality and its application to a fractional differential equation. *J. Math. Anal. Appl.* **2007**, *328*, 1075–1081. [[CrossRef](#)]
33. Xie, S.S.; Li, G.X.; Yi, S. Compact finite difference schemes with high accuracy for one-dimensional nonlinear Schrödinger equation. *Comput. Methods Appl. Mech. Eng.* **2009**, *198*, 1052–1060. [[CrossRef](#)]
34. Sun, Z.; Zhao, D. On the l^∞ convergence of a difference scheme for coupled nonlinear Schrödinger equations. *Comput. Math. Appl.* **2010**, *59*, 3286–3300. [[CrossRef](#)]
35. Lv, S.Q.; Nie, Z.H.; Liao, C.C. Stability and Convergence Analysis of Multi-Symplectic Variational Integrator for Nonlinear Schrödinger Equation. *Mathematics* **2023**, *11*, 3788. [[CrossRef](#)]
36. Wang, D.; Xiao, A.; Yang, W. A linearly implicit conservative difference scheme for the space fractional coupled nonlinear Schrödinger equations. *J. Comput. Phys.* **2014**, *272*, 644–655. [[CrossRef](#)]
37. Pan, K.J.; Zeng, J.L.; He, D.D.; Zhang, S.Y. A fourth-order difference scheme for the fractional nonlinear Schrodinger equation with wave operator. *Appl. Anal.* **2022**, *101*, 2886–2902. [[CrossRef](#)]

Disclaimer/Publisher's Note: The statements, opinions and data contained in all publications are solely those of the individual author(s) and contributor(s) and not of MDPI and/or the editor(s). MDPI and/or the editor(s) disclaim responsibility for any injury to people or property resulting from any ideas, methods, instructions or products referred to in the content.